

Topological phase transition of $\text{Bi}_{2-x}\text{In}_x\text{Te}_3$

Q. JING^{1,2}, W. X. JIANG^{1,3}, Z. Q. YANG^{1,3}, J. F. WANG², M. Y. YAO^{1,3}, F. F. ZHU^{1,3}, Y. L. LI^{1,3}, S. B. LI^{1,3}, J. Y. HU^{1,3}, C. H. XU^{1,3}, B. LIU² and D. QIAN^{1,3(a)}

¹ Key Laboratory of Artificial Structures and Quantum Control (Ministry of Education), Shenyang National Laboratory for Materials Science, School of Physics and Astronomy, Shanghai Jiao Tong University - Shanghai 200240, China

² Laboratory of Functional Molecules and Materials, School of Physics and Optoelectronic Engineering, Shandong University of Technology - 266 Xincun Xi Road, Zibo, 255000, China

³ Tsung-Dao Lee Institute, Shanghai Jiao Tong University - Shanghai 200240, China

received 30 August 2019; accepted in final form 15 November 2019

published online 10 January 2020

PACS 79.60.-i – Photoemission and photoelectron spectra

PACS 73.20.-r – Electron states at surfaces and interfaces

PACS 73.20.At – Surface states, band structure, electron density of states

Abstract – Compared with Bi_2Se_3 with its Dirac point in the bulk gap, the Dirac point of Bi_2Te_3 is in the valence band, then it is generally considered that it is difficult to observe the topological phase transition course in the Bi_2Te_3 system via nonmagnetic lighter element doping. Here, we report the phase transition of $\text{Bi}_{2-x}\text{In}_x\text{Te}_3$, from a topological insulator to a trivial band insulator observed by angle-resolved photoemission spectroscopy. The robust surface state exists in the range of $x \sim 0.1$. At $x = 0.3$, the surface state completely disappears and only the bulk gap exists, suggesting a sudden gap closure and topological phase transition around $x = 0.1-0.3$.

Copyright © EPLA, 2020

Introduction. – Induced by spin-orbit coupling (SOC), topological insulators (TIs) have insulating energy gaps in the bulk, and gapless edge or surface states on the sample boundary that are protected by time-reversal symmetry [1,2]. A three-dimensional (3D) TI has gapless surface state with Dirac cone-shaped band dispersion around time-reversal invariant points of surface Brillouin zone [3,4]. However, the topological character of topological insulators is determined by the nature of their valence-band wave functions, which can be quantified by Z_2 invariant [5]. As one of the important 3D topological insulators, Bi_2Te_3 owns a bandgap of 165 meV, which is larger than the thermal energy at room temperature [6]. Compared to Bi_2Se_3 with Dirac point in the bulk gap, the Dirac point of Bi_2Te_3 is located at the top of the bulk valence band, which makes it more difficult to separate the contribution to transport of the hole part of the Dirac surface states, from that due to the bulk valence band [7]. However, the location of the Dirac point of Bi_2Te_3 makes it possess an advantage over Bi_2Se_3 in terms of tunability of the Dirac point energy [8,9]. On the aspect of application, Bi_2Te_3 can be utilized to fabricate a $\text{Bi}_2\text{Te}_3/\text{NbSe}_2$ heterostructure to realize topological

superconductivity [10] according to the proximity effect, then to investigate the Majorana zero mode [11]. Bi_2Te_3 could also be as the substrate to grow the single-bilayer $\text{Bi}(111)$ ultrathin film, which shows two-dimensional quantum spin Hall state [12].

For topological phase transition, the alloying of known topological insulators with lighter elements, by tuning SOC or lattice constant can cause the bulk bandgap to close and invert at a critical point where the topological class changes [5]. Until now, 3D topological phase transition induced by nonmagnetic lighter element doping has been realized in experiment, mainly in $\text{TlBi}(\text{S}_{1-x}\text{Se}_x)_2$ and $\text{Bi}_{2-x}\text{In}_x\text{Se}_3$ systems. For $\text{TlBi}(\text{S}_{1-x}\text{Se}_x)_2$, the existence of a critical point between the topological insulator TlBiSe_2 and the trivial metal TlBiS_2 is observed [13–17]. For $\text{Bi}_{2-x}\text{In}_x\text{Se}_3$, Brahlek *et al.* [18] reported its transformation from a topologically nontrivial metal into a topologically trivial band insulator by combining transport and photoemission measurements on $\text{Bi}_{2-x}\text{In}_x\text{Se}_3$ thin films. Lou *et al.* [19] studied the phase transition of $\text{Bi}_{2-x}\text{In}_x\text{Se}_3$ from a topological insulator to a trivial band insulator using angle-resolved photoemission spectroscopy (ARPES) on $\text{Bi}_{2-x}\text{In}_x\text{Se}_3$ single crystals. They reported the complete evolution of the bulk band structures throughout the transition and discussed the mechanism of the phase

^(a) E-mail: dqian@sjtu.edu.cn

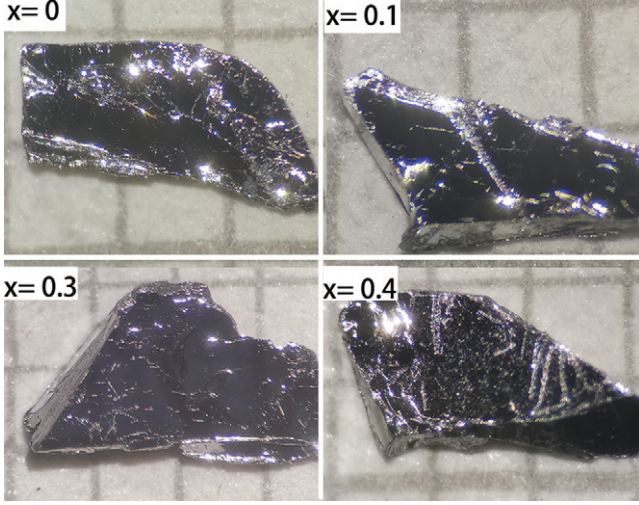


Fig. 1: The crystal morphology of the $\text{Bi}_{2-x}\text{In}_x\text{Te}_3$. The scale is in millimeters.

transition, proposing that it was governed by the combined effect of spin-orbit coupling and interactions upon band hybridization. For Bi_2Te_3 , as its Dirac point is located at the top of bulk valence band, then it is generally considered that it is difficult to observe its phase transition process by nonmagnetic lighter element doping. Here, we report the phase transition of $\text{Bi}_{2-x}\text{In}_x\text{Te}_3$, from a topological insulator to a trivial band insulator observed by ARPES on $\text{Bi}_{2-x}\text{In}_x\text{Te}_3$ single crystals. Meanwhile, we have observed the moving of its Dirac point.

Methods. – Similar to the growth of $\text{Bi}_{2-x}\text{In}_x\text{Se}_3$, high-quality single crystals of $\text{Bi}_{2-x}\text{In}_x\text{Te}_3$ were grown by slowly cooling a stoichiometric mixture of high-purity elements of bismuth, indium, and tellurium in an evacuated quartz tube [20]. The ARPES measurements were performed using 70–100 eV photons at Advanced Light Source beamline 4.0.3 using Scienta R4000 analyzer with base pressure better than 5×10^{-11} torr. Energy resolution was better than 15 meV and angular resolution was better than 0.02° . Different polarization light was used to reduce the matrix element effect in the ARPES measurement [21]. The position of the Fermi level was referenced to a copper plate in electrical contact with the samples. No charging effect was observed during measurements at low temperatures.

Results and discussion. – As shown in fig. 1, all samples are easily cleaved along the basal plane, leaving a silvery shining mirror-like surface. First, we utilize peak area sensitive factor method to investigate the indium doping amount roughly. According to the method, the generalized expression for determination of the atom fraction of any constituent in a sample can be written as an expression $[A]\text{atom}\% = (I_A/F_A)/\sum(I/F) \times 100\%$. Here, “A” is the name of the element investigated; “F” is defined as atomic sensitivity factor; “I” denotes the

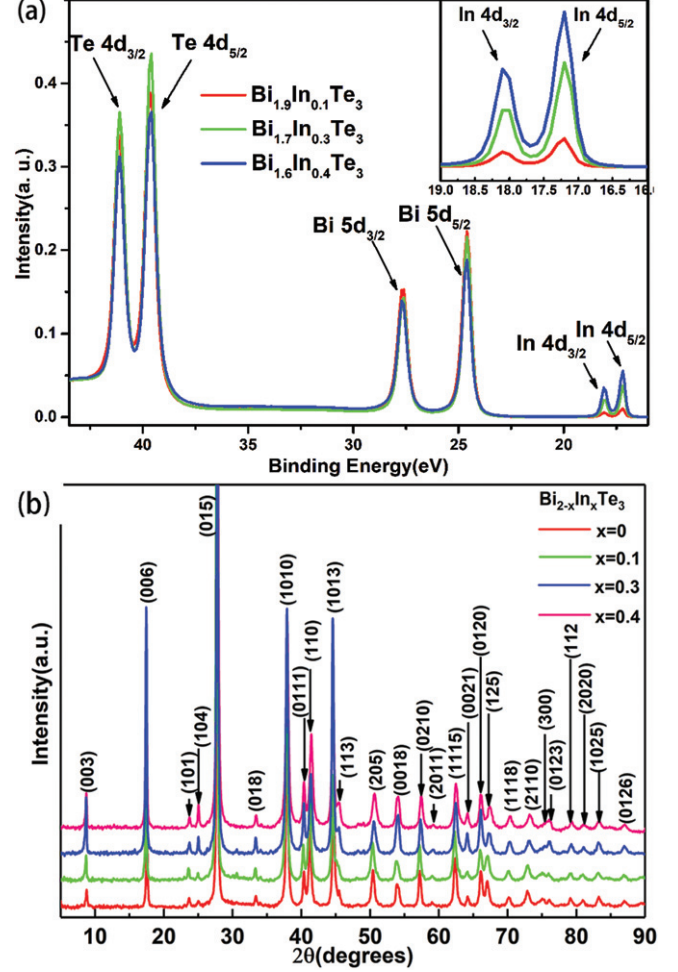


Fig. 2: (a) The normalized core-level photoemission spectrum of $\text{Bi}_{2-x}\text{In}_x\text{Te}_3$ with $x = 0.1, 0.3, 0.4$, respectively. The peak of indium element is present in the spectra, suggesting that the indium element has been doped into Bi_2Te_3 . The excitation energy is 94 eV for all samples. (b) The powder XRD pattern of $\text{Bi}_{2-x}\text{In}_x\text{Te}_3$.

peak area in the spectrum; \sum means to do summation for all elements in the sample [22]. Therefore, the atom number ratio of In to Bi, could be expressed as $R_{\text{In/Bi}} = (I_{\text{In}}/F_{\text{In}})/(I_{\text{Bi}}/F_{\text{Bi}}) = (I_{\text{In}}/I_{\text{Bi}})/(F_{\text{In}}/F_{\text{Bi}}) = (I_{\text{In}}/I_{\text{Bi}}) \times C$, in which both F_{In} and F_{Bi} could be considered as constants. Therefore, we could investigate the indium doping amount by comparing the peak area of indium and bismuth in the spectrum, directly. Here, we utilize the peak area of $\text{In } 4d_{5/2}$ and $\text{Bi } 5d_{5/2}$ to reflect the indium doping amount. According to fig. 2(a), we find that the peak area ratio of $\text{In } 4d_{5/2}$ to $\text{Bi } 5d_{5/2}$ increases with the increase of nominal doped amount of $x = 0.1, 0.3, 0.4$. Figure 2(b) shows the XRD pattern of all four samples. It is evident that all the samples are isostructural to the parent compound Bi_2Te_3 , which has rhombohedral structure belonging to $D_{3d}^5(R\bar{3}m)$ space group, *i.e.*, there exists no impurity phase in $\text{Bi}_{2-x}\text{In}_x\text{Te}_3$ samples. It suggests that In atoms have substituted Bi atoms completely.

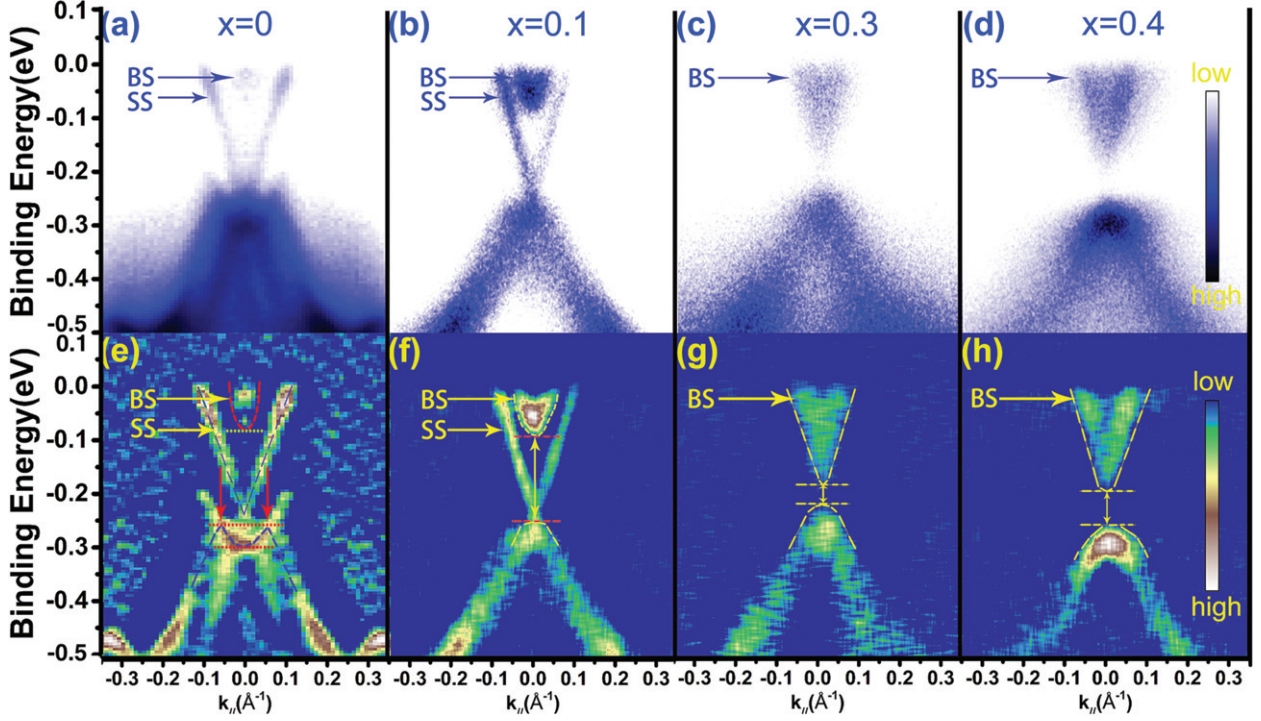


Fig. 3: Panels (a)–(d) show the band dispersions of a series of doped samples along the $\bar{\Gamma}$ – \bar{M} direction. Panels (e)–(h) show the corresponding second-derivative plots of panels (a)–(d). The ARPES k_{\parallel} maps of Bi_2Te_3 and $\text{Bi}_{2-x}\text{In}_x\text{Te}_3$ are obtained using incident photon energy of 74 eV and 86 eV, respectively. For $\text{Bi}_{2-x}\text{In}_x\text{Te}_3$, the nominal composition values are noted on the samples. Owing to the k_z dispersion of the bulk bands, the true gap is likely to be smaller than these estimates. The bulk states and surface states are marked out. BS denotes the bulk states, while SS corresponds to surface states.

As shown in fig. 3, the bands evolution of $\text{Bi}_{2-x}\text{In}_x\text{Te}_3$ is illustrated by its in-plane electronic structure (E_B vs. k_{\parallel}) at varying compositions (x). It is evident that the two end compounds ($x = 0$ and 0.4) are in clear contrast, namely, $x = 0$ has surface states connecting the bulk conduction and valence bands, while $x = 0.4$ has no surface states, which clearly reveals the difference between the conventional semiconductor phase and the Z_2 topological band insulator phase. The topological state is clearly observed from $x = 0.0$ to 0.1 , where the bulk conduction and valence bands are separated by an observable bulk gap, which is traversed by the gapless topological surface states. Thus, our data show that the system belongs to the topological insulator regime for compositions of $x \leq 0.1$. However, when $x \geq 0.3$, there exists no surface state anymore.

As the surface state of Bi_2Te_3 is two-dimensional, even the photoemission spectra of pure Bi_2Te_3 collected with different excitation light from that of indium-doped samples, it could still help us to understand the band evolution process. For the topologically nontrivial region, the bulk gap is defined as the difference between the conduction band minimum (CBM) and the valley of valence band (VB) at the Γ point. For the topologically trivial region, the bulk gap corresponds to the difference between the CBM and valence band maximum (VBM). In the topologically nontrivial region, the magnitude of bulk gap is 0.21 eV for $x = 0$. The valley structure in VB, caused by

the band inversion, gradually weakens along with the increasing doping. As marked out by arrows in fig. 3(e), the absolute values of δk 's is 0.113 \AA^{-1} for pure Bi_2Te_3 . When x reaches the value of 0.1 in $\text{Bi}_{2-x}\text{Te}_2\text{In}_x$ system, it is difficult to distinguish the valley structure of VB. The weakening of valley structure in VB with the increasing doping demonstrates the decrease of SOC strength [19]. Based on that, here, we think the gap of $\text{Bi}_{1.9}\text{Te}_2\text{In}_{0.1}$ is equal to the value of difference between CBM and VBM directly, which is 159 meV. In the topologically trivial region, the band inversion disappears and the valley structure vanishes too. A bulk bandgap of $E_g = 38$ meV is observed for $x = 0.3$ in fig. 3(g), indicating that the system starts to become the conventional semiconductor phase. For $x = 0.4$, the energy gap reaches up to 63 meV. The increase of the direct band gap indicates the further decrease of SOC strength [23–25].

Based on the evolution of band structures of $\text{Bi}_{2-x}\text{In}_x\text{Te}_3$, a local phase transition characterized with a sudden gap closure happens around $x \sim 0.1$ – 0.3 . Meanwhile, the movement of Dirac point (DP) toward the CBM with the increasing doping is observed too. It should be pointed out that, different from that of $\text{Bi}_{2-x}\text{In}_x\text{Se}_3$, the location of Dirac point of $\text{Bi}_{2-x}\text{In}_x\text{Te}_3$ has moved from the valence band to the top of the valence band. A schematic drawing depicting the evolution of the bulk gap is shown in fig. 4. As shown in the shadow region of fig. 4(c), the

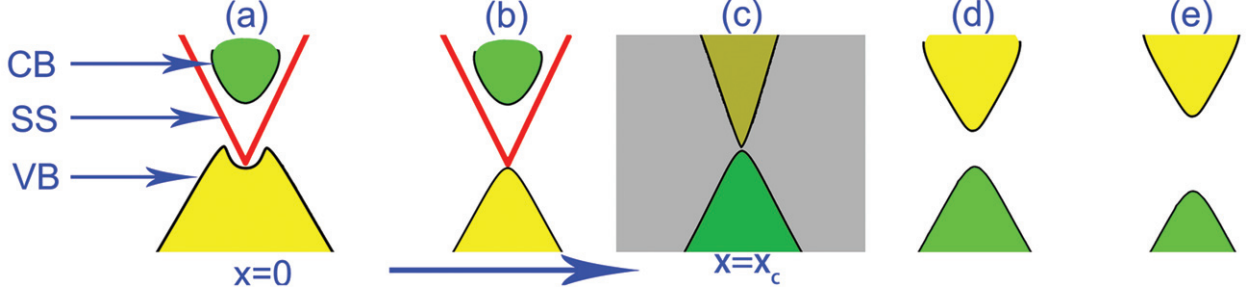


Fig. 4: A schematic picture of the band structure evolution of $\text{Bi}_{2-x}\text{In}_x\text{Te}_3$ as a function of In concentration. The different colors of the bulk bands represent different orbital characters and parities.

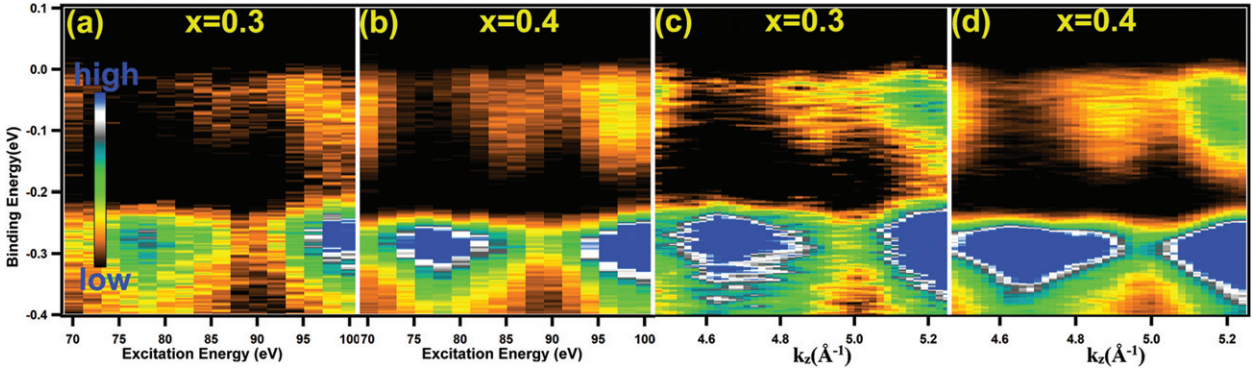


Fig. 5: Panels (a) and (b) show the incident photon energy-dependence spectra for $\text{Bi}_{2-x}\text{In}_x\text{Te}_3$, with $x = 0.3$ and 0.4 , respectively. The incident photon energy is from 70 to 100 eV for all samples. Panels (c) and (d) show the k_z dependence spectra of $\text{Bi}_{2-x}\text{In}_x\text{Te}_3$, with $x = 0.3$ and 0.4 , respectively. The k_z range shown for $\delta k = 0.78 \text{ \AA}^{-1}$ corresponds to the incident photon energy from 70 to 100 eV.

gap size has a dramatic transformation between $x = 0.1$ and 0.3 , which means that a critical transition has happened. Striding across the critical point, a strong increase of the band gap from $x = 0.3$ to 0.4 is observed. It is well accepted that the band inversion is induced by SOC for a 3D topological insulator [26]. When SOC is turned on, it will induce the conduction band (CB) and VB shifting downward and upward, respectively, resulting in the band inversion in the topologically nontrivial region. Then, owing to the interactions within the overlap, the bulk gap would reopen. In summary, the combined effect of SOC and interactions upon band hybridization together tune the band gap involution, leading the topological phase transition.

As shown in fig. 5, to better understand the nature of the band structure of $\text{Bi}_{2-x}\text{In}_x\text{Te}_3$, we perform ARPES measurements as a function of incident photon energy on $\text{Bi}_{2-x}\text{In}_x\text{Te}_3$ with $x = 0.3$ and 0.4 , respectively. For $\text{Bi}_{1.7}\text{In}_{0.3}\text{Te}_3$, within the incident photon energy of 70–94 eV, it could be observed that the gap is open. However, within the incident photon energy of 94–100 eV the gap seems closed. To verify whether the gap is open or not, we investigate pictures one by one with increasing incident photon energy from 94–100 eV. Corresponding to the incident photon energy of 94 eV, 96 eV, 98 eV, 100 eV, the bulk gap of $\text{Bi}_{1.7}\text{In}_{0.3}\text{Te}_3$ is about 38, 63, 43, 49 meV,

respectively, according to the second-order derivative results (see figures included in the Supplementary Material [SupplementaryMaterial.pdf](#) (SM)¹). For $\text{Bi}_{1.6}\text{In}_{0.4}\text{Te}_3$, it could be observed clearly that the gap is open in the full range. Furthermore, to confirm the photon-energy range (70–100 eV) is broad enough to cover one unit Brillouin zone at least, the k_z dependence spectra are gotten after conversion. According to k_z dependence spectra of fig. 5(c) and (d), δk_z is about 0.78 \AA^{-1} , while the period of k_z for one Brillouin zone is about 0.617 \AA^{-1} , then the range of the excitation photon energy we have taken corresponds to 1.2 unit Brillouin zone. Thus, to sum up the points which we have just raised, when doping amount reaches up to $x = 0.3$ nominally, the gap has opened and surface state has disappeared, *i.e.*, $\text{Bi}_{2-x}\text{In}_x\text{Te}_3$ has translated into topologically trivial insulator completely. We think the band evolution mechanism of $\text{Bi}_{2-x}\text{In}_x\text{Te}_3$ is similar with that of $\text{Bi}_{2-x}\text{In}_x\text{Se}_3$ [19]. Figure 4 shows schematic drawing of the band structure evolution in the topological phase transition process. In the topologically nontrivial region ($x < x_c$), there exists band inversion, and thus the band hybridization and SOC together modulate the bulk-gap size, causing the bulk gap not to change

¹See the SM for the incident photon energy-dependence spectra of $\text{Bi}_{1.7}\text{In}_{0.3}\text{Te}_2$. The photon energy is marked on the top of the spectra.

significantly. With the increase of In doping, the overlap between the CB and VB becomes weak. At the critical point ($x = x_c$), the band inversion vanishes, as does the band hybridization, and the bulk gap collapses, accompanied by the vanishing of the surface state. In the topologically trivial region ($x > x_c$), the further decreasing SOC strength makes the CB and VB separated, giving rise to the increase of bulk gap.

This work was supported by the Ministry of Science and Technology of China (Grant No. 2016YFA0301003), the National Natural Science Foundation of China (Grants No. U1632272, No. 11574201, No. 11521404, No. 11804194) and Natural Science Foundation of Shandong Province, China (No. ZR2016AQ08). DQ acknowledges support from the Changjiang Scholars Program and a Shanghai talent program. The Advanced Light Source is supported by the Director, Office of Science, Office of Basic Energy Sciences, of the US Department of Energy under Contract No. DE-AC02-05CH11231.

REFERENCES

- [1] HASAN M. Z. and KANE C. L., *Rev. Mod. Phys.*, **82** (2010) 3045.
- [2] QI X.-L. and ZHANG S.-C., *Rev. Mod. Phys.*, **83** (2011) 1057.
- [3] FU L., KANE C. L. and MELE E. J., *Phys. Rev. Lett.*, **98** (2007) 106803.
- [4] HSIEH D., QIAN D., WRAY L., XIA Y., HOR Y. S., CAVA R. J. and HASAN M. Z., *Nature (London)*, **452** (2008) 970.
- [5] WU L., BRAHLEK M., AGUILAR R. V., STIER A. V., MORRIS C. M., LUBASHEVSKY Y., BILBRO L. S., BANSAL N., OH S. and ARMITAGE N. P., *Nat. Phys.*, **9** (2013) 410.
- [6] SHEN SHUN-QING, *Topological Insulators: Dirac Equation in Condensed Matter*, Springer Series in Solid-State Sciences, second edition, Vol. **187** (Springer, Singapore) 2017, ISBN 978-981-10-4606-3, DOI 10.1007/978-981-10-4606-3.
- [7] FRANZ MARCEL and MOLENKAMP LAURENS, *Topological Insulators*, in *Contemporary Concepts of Condensed Matter Science*, Vol. **6** (Elsevier) 2013, ISSN: 1572-0934.
- [8] WANG L., HUANG M., THIMMAIAH S., ALAM A., BUD'KO S. L., KAMINSKI A., LOGRASSO T. A., CANFIELD P. and DUANE D. JOHNSON, *Phys. Rev. B*, **87** (2013) 125303.
- [9] SCANLON D. O., KING P. D. C., SINGH R. P., DE LA TORRE A., MCKEOWN WALKER S., BALAKRISHNAN G., BAUMBERGER F. and CATLOW C. R. A., *Adv. Mater.*, **24** (2012) 2154.
- [10] XU J. P., LIU C. H., WANG M. X., CHEN Y., LIU Y., XU Z. A., GAO C. L., QIAN D., ZHANG F. C., JIA J. F. *et al.*, *Phys. Rev. Lett.*, **112** (2014) 217001.
- [11] SUN H. H., ZHANG K. W., LI Y. Y., LIU C., QIAN D., ZHOU Y., FU L., LI S. C., ZHANG F. C., JIA J. F. *et al.*, *Phys. Rev. Lett.*, **116** (2016) 257003.
- [12] HIRAHARA T., BIHLMAYER G., SAKAMOTO Y., YAMADA M., MIYAZAKI H., KIMURA S., S. BLÜGEL and HASEGAWA S., *Phys. Rev. Lett.*, **107** (2011) 166801.
- [13] SATO T., SEGAWA K., KOSAKA K., SOUMA S., NAKAYAMA K., ETO K., MINAMI T., ANDO Y. and TAKAHASHI T., *Nat. Phys.*, **7** (2011) 840.
- [14] XU S., XIA Y., WRAY L., DIL J. H., OSTERWALDER J., SLOMSKI B., BANSIL A., LIN H., CAVA R. J., HASAN M. Z. *et al.*, *Science*, **332** (2011) 560.
- [15] CHEN Y. L., LIU Z. K., ANALYTIS J. G., CHU J. H., ZHANG H. J., LU D. H., FISHER I. R., ZHANG S. C., HUSSAIN Z., SHEN Z. X. *et al.*, *Phys. Rev. Lett.*, **105** (2010) 266401.
- [16] SOUMA S., KOMATSU M., NOMURA M., SATO T., TAKAYAMA A., TAKAHASHI T., ETO K., SEGAWA K. and ANDO Y., *Phys. Rev. Lett.*, **109** (2012) 186804.
- [17] XU S., NEUPANE M., BELOPOLSKI I., LIU C., ALIDOUST N., BIAN G., JIA S., LANDOLT G., BANSIL A., HASAN M. Z. *et al.*, *Nat. Commun.*, **6** (2015) 6870.
- [18] BRAHLEK M., BANSAL N., KOIRALA N., XU S. Y., NEUPANE M., LIU C., HASAN M. Z. and OH S., *Phys. Rev. Lett.*, **109** (2012) 186403.
- [19] LOU R., QIAN T., DING H. and WANG S., *Phys. Rev. B*, **92** (2015) 115150.
- [20] ANALYTIS J. G., CHU J. H., CHEN Y. L., CORREDOR F., McDONALD R. D., SHEN Z. X. and FISHER I. R., *Phys. Rev. B*, **81** (2010) 205407.
- [21] HAN C. Q., YAO M. Y., ZHU F. F. and QIAN D., *Phys. Rev. B*, **90** (2014) 085101.
- [22] WAGNER C. D., RIGGS W. M., DAVIS L. E., MOULDER J. F. and MUILENBERG G. E., *Handbook of X-ray Photoelectron Spectroscopy* (Perkin-Elmer Corporation) 1979.
- [23] ZHANG H., LIU C.-X., QI X.-L., DAI X., FANG Z. and ZHANG S.-C., *Nat. Phys.*, **5** (2009) 438.
- [24] BERNEVIG B. A., HUGHES T. L. and ZHANG S.-C., *Science*, **314** (2006) 1757.
- [25] ZAHID HASAN M. and MOORE JOEL E., *Annu. Rev. Condens. Matter Phys.*, **2** (2011) 55.
- [26] ZHANG H., LIU C., QI, X., DAI X., FANG Z. and ZHANG S., *Nat. Phys.*, **5** (2009) 438.